J. Mol. Model. **1997**, *3*, 443 – 454

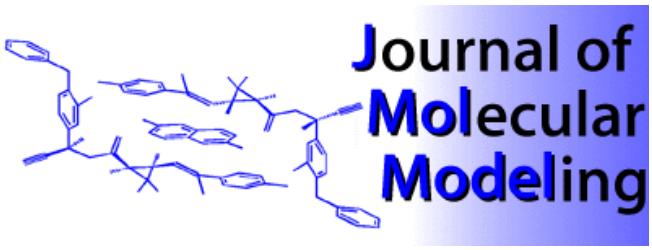

Docking of a Series of Peptide-Based Interleukin-1β Converting Enzyme Inhibitors with Aspartyl Hemiacetals, α-((2,6-Dichlorobenzoyl)oxy)methyl and (Acyloxy)methyl Ketone Moieties

Vankayalapati Hariprasad, and Vithal M. Kulkarni*

Pharmaceutical Division, Department of Chemical Technology, University of Mumbai, Matunga, Mumbai - 400019, India (kulkarni@giasbma.vsnl.net.in)

Received: 21 January 1997 / Accepted: 14 October 1997 / Published: 30 October 1997

Abstract

The enzyme-binding mode of a series of interleukin-1β converting enzyme (ICE) inhibitors has been analysed on the basis of the crystal structure of the complex between hICE and tetrapeptide aldehyde. The conformation of these ligands were explored by performing molecular dynamics simulations at 100 ps. The conformation adopted by these inhibitors was very similar to and could be superimposable onto the regions of crystal structure. The active and the low energy conformers were docked either by grid or manually into the binding site. The analysis of the resulting model indicated that O-benzylacyl group of aspartyl hemiacetals interact with Cys285 and the large substituents: semicarbazone, 2,6-bis(trifluoromethyl) benzoate, other leaving groups of (acyloxy)methyl and α-((2,6-dichlorobenzoyl)oxy)methyl ketone series of **P1** site protrude from the surface of Cys285 and interact with Val338, which is located below the binding pocket. The hydrogen bonding interaction between -NH of semicarbazone and Cys285 seems to have significant role. The total potential energy including intermolecular interaction energy, consisting of van der Waals and electrostatic energies were calculated. The resulting model is qualitatively consistent with the reported experimental data and can be useful for the design of more potent inhibitors of ICE.

Keywords: Cysteine protease, Peptide-based ICE inhibitors, Docking analysis

Introduction

Human interleukin-1β converting enzyme (hICE) a heterodimer consists of two subunits with molecular weights of 20 kDa (p20) and 10 kDa (p10) and is a processing cysteine protease enzyme [1-3]. It requires an aspartate at **P1** for enzyme specificity [4], to cleave the biologically inactive 31 kDa precursor interleukin-1β (pro-IL-1β) at the sequence-related site: Asp27-Gly28 (site 1) and Asp116-Ala117 (site 2) resulting in the generation of mature, 17.5 kDa biologically active inflammatory cytokine interleukin-1β [5,6] (IL-1β). Inhibition of hICE prevents cleavage of IL-1β which is a potential mechanism for reducing IL-1 activity and may present an attractive target for anti-inflammatory agents [7] to treat chronic inflammatory diseases such as rheumatoid arthritis, septic shock, inflammatory bowel disease and other physiological conditions including wound healing [8-10],

* *To whom correspondence should be addressed*

growth of certain leukemia [11] and apoptosis [12]. Tetrapeptide corresponding to the substrate **P4-P1** residue (Figure 1) for specific recognition has led to the design of several potent inhibitors of ICE [13-17]. Thiol alkylating agents [3], compounds from substructure similarity search [18] and a cytokine response modifier gene the *crm A* found in cowpox virus [19] inhibit ICE activity. Three-dimensional structures of hICE in complex with tetrapeptide aldehyde and chloromethyl ketone inhibitors [20,21], the mechanism of ICE catalysis involving a catalytic dyad His237 and Cys285 and "oxyanion hole" Gly238 and Cys285 have provided a considerable insight into the structural features of these complexes.

In this paper, we report the application of grid or manual docking method to the three series of ligands: aspartyl hemiacetals, α-((2,6-dichlorobenzoyl)oxy)methyl and (acyloxy)methyl ketone containing moieties [22-24] to elucidate their binding mode with ICE and to explain the known structure-activity data that might be useful for the design of more potent inhibitors of ICE.

Methodology

The 3D structure of interleukin-1β converting enzyme complexed with a tetrapeptide aldehyde inhibitor (acetyl-Tyr-Val-Ala-Asp-H) [25] (entry 1ice in the Brookhaven Protein Data Bank) was used in this study. Inhibitor covalently bound to Cys285 and X-ray water molecules were removed and all hydrogens were supplied and positions were refined till the convergence was reached, while constraining the heavy atoms. In the next stage, the α-carbon atoms of the model were constrained to remain as close as possible to the corresponding α-carbon atoms of X-ray structure. Once the positions of all atoms of the protein were computed, the entire molecule was subjected to energy minimization in which constraints of the α-carbon atoms were gradually removed. Calculations were done using the steepest descent and conjugate gradient minimization algorithms. The resulting structure subsequently served as the starting structure for further energy refinement, docking and complex formation.

The compounds in this study with their ICE inhibitory activity are given in Table 1–3. Each of the ligands were built using the crystal structure of tetrapeptide aldehyde and energy minimized. Partial charges were assigned to the enzyme and ligands by Gasteiger method. The systematic conformational search was performed on each of the minimized ligands using 100 ps molecular dynamics simulations as reported previously [26] at 300 K. Dynamics were equilibrated for 10 ps with time step of 1 fs and continued for 100 ps simulations. The resulting low energy structure was extracted and energy minimized to 0.001 kcal/mol·Å. The non-bonded cutoff distance of 8 Å and a distant dependent dielectric constant (e = 4rij) [27] was employed. All calculations were performed on a Silicon Graphics INDY R4400 workstation (Silicon Graphics Inc., USA). CVFF [28] implemented in Discover version 2.9.5 was used for all the molecular mechanics calculations and model building were performed using INSIGHT II [29] (version 2.3.5) molecular modeling software.

Docking Procedure

To find a sterically reasonable binding geometries for specific interactions of a ligand in the active site pocket, the docking option available within the INSIGHT II was used. The lowest potential energy conformers from molecular dynamics simulations were taken to be the best candidates for the grid-docking experiments. The conformers with probable H-bonding were placed in the enzyme cavity by superposition of similar heteroatoms with those of the reference frame (crystal structure). The origin of this reference frame is situated in the active site pocket of ICE. Employing interactive docking procedure, ligands were docked into the enzyme active site. Prior to docking, the regions allowed to accommodate ligand molecules were indicated by a rectangular box using create docking grid for whole ligand-binding region for each molecule. The energy docking grid that represents the potential energy of the enzyme at a finite point in space was computed by calculating the interaction energy between the atom of the moving molecule and the grid points using the following expression as:

$$E = \sum_j q_i \sum_{i \in r_{ij}} \underline{q_j} + \sum_j \sqrt{A_j} \sum_i \frac{\sqrt{A_j}}{r_{ij}^{12}} - \sum_j \sqrt{B_j} \sum_i \frac{B_i}{r_{ij}^{6}}$$

the quantity r_{ij} can be rewritten as r_{ig} , r_{ig} = the distance between the grid point and the atom in the non-moving molecule. In order to clarify the orientation of the ligands in the active site, the electrostatic potential at van der Waals surface were computed using solvent surface calculations. Thus the orientation with low intermolecular potential energy was obtained (best force field score) by moving the ligand molecule slowly into the active site and updating the interaction energy continuously. After docking, the complex structure was energy minimized by applying constraints to hydrogen bonded atoms in the active site. Finally, the whole system was relaxed to low rms value by using conjugate gradient method.

Results and Discussion

Figure 2 shows the active site of energy minimized complex of aspartyl hemiacetal corresponding to **5** and its mode of binding with ICE. The interaction between Arg341-NH...O Val, Arg341-O...HN and oxyanion O of -C=O Val atoms of aspartyl hemiacetals containing benzyloxycarbonyl (**4**) are responsible for specific recognition of the substrate by enzyme. The intermolecular hydrogen bonding to residue Gly238 located in the "oxyanion hole" with acceptor carbo-

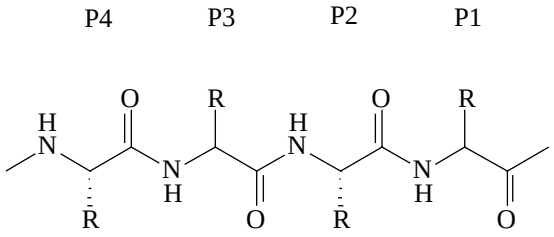

Figure 1. *Critical binding sites of the crystal structure of tetrapeptide aldehyde inhibitor of ICE along with the peptide back bone residues. P1, aspartic acid; P2, alanine; P3, valine; P4, tyrosine.*

nyl group (2.06 Å) of **P1** aspartate may be stabilized by active site His237. However, the donor group Val-NH take part in strong hydrogen bonding interaction with the oxygen atom of Arg341. This residue is well defined site in most of the conformers of the ligand **4**. The terminal benzyloxycarbonyl (Z) group positioned in the **P4** site exhibits similar type of conformation to that of Tyr residue as present in the crystal structure. The complexes of cyclic hemiacetal **5** and semicarbazone derivative **7** with ICE confirmed the results of binding orientation of the reported peptide aldehyde complex structure. The oxyanion and ring oxygen of ligand **5** interact with Gly238 and His237 which have strong hydrogen bonding with distances 2.76 and 1.83 Å between His237-ND1...O of Asp and Gly238-NH...O of carbonyl oxygen respectively. Another important finding of docking studies suggest that -N- atom of semicarbazone (SC) functionality seems to have significant role in hydrogen bonding interaction with SG atom of Cys285.

It is interesting to note that the cyclic hemiacetals of aspartyl equivalent group exhibit more stable docking conformation than that of the aspartate alone. The back bone conformation of **5** in the most stable orientation is very close to that of complex crystal structure. The change through the docking experiments seen in the torsion angle of C2-C3-N4-C5, O-C5-C6-N7, vary by about 30.1 and 70.5°. This difference is due to the cyclic aspartyl equivalent at **P1** site or position of oxyanion and semicarbazone groups. From the structure-activity data of the compounds **1** and **3** (Table 1), the hydrogen bonding interaction of carbonyl group at **P1** site with Gly238 and Cys285 is essential for activity. The interaction energy of the most stable docking models shown in Table IV explain the high activity of ligands **5** and **7**. Thus the present study identifies the role of 'oxyanion ' in the binding mode of **5**. It was reasoned from this study that the hydroxyl group present in the cyclic hemiacetals participate in the hydrogen bonding formation with the enzyme and is essential for activity.

In α-((2,6-dichlorobenzoyl)oxy)methyl ketone **9** (Table 2) the absence of hydrogen bonding interaction with Gly238 is due to orientation of 2,6-dichlorobenzoyloxy functionality deep in the pocket involved with Val338 and made a way for oxyanion which bind with Ser339 through hydrogen bonding interaction as depicted in Figure 3. The 2,6-dichlorobenzoyloxy carbonyl group forms strong hydrogen bond with

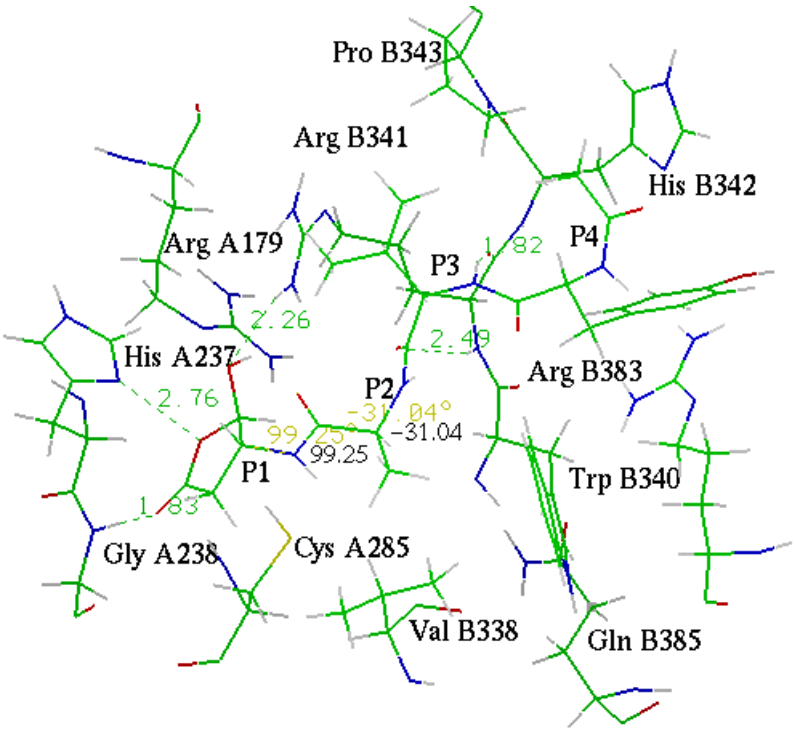

Figure 2. *Binding mode of most stable docking model of ICE/inhibitor **5** complex containing-aspartyl aldehyde moiety. The active site residues of hICE involved in hydrogen bonding interactions are shown in dashed lines. The change in torsion angle of C2-C3-N4-C5 (99.0) and O-C5-C6-N7 (-31.04) are also shown.*

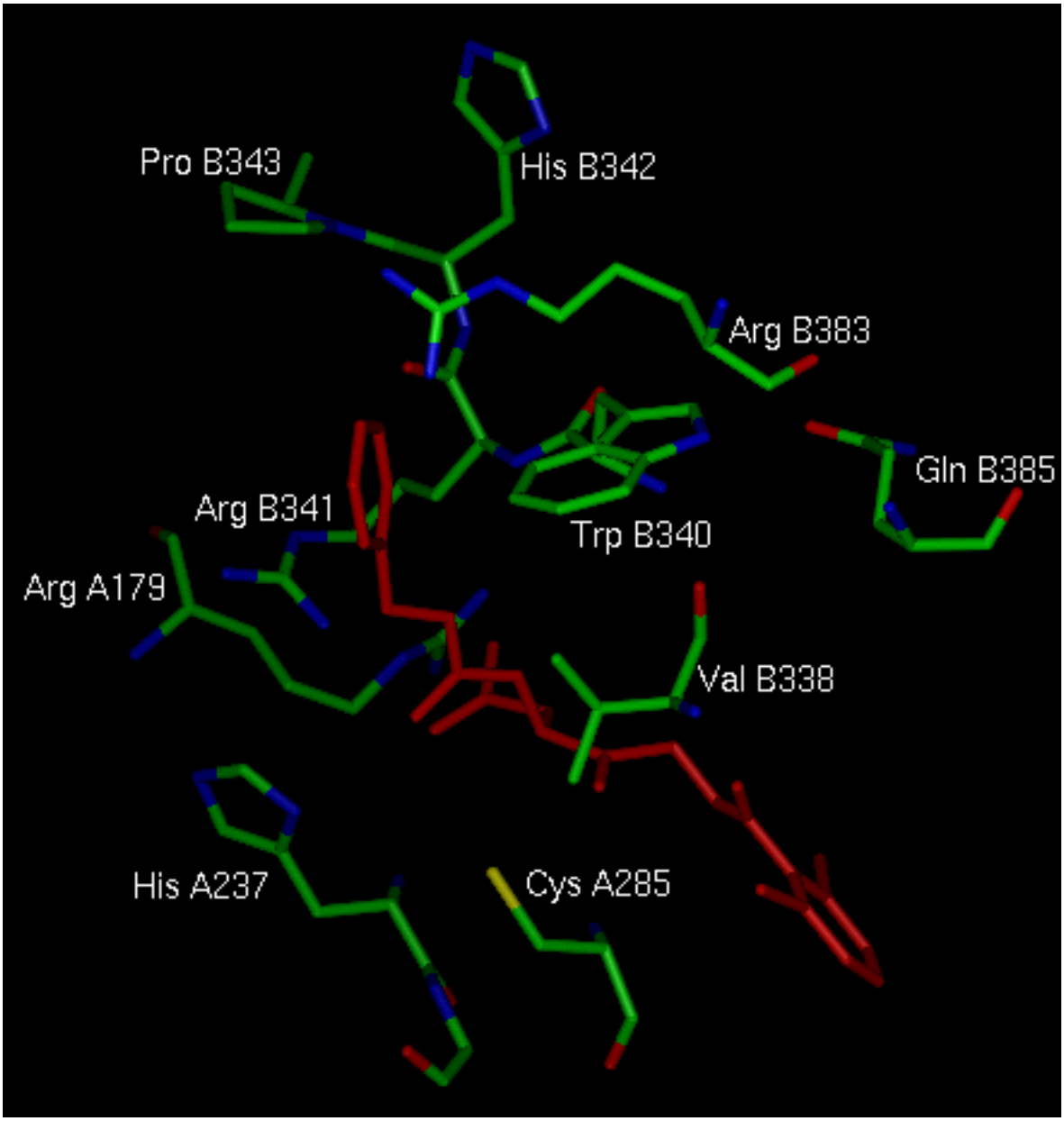

Figure 3. *The minimized energy structure of ICE/#a-((2,6-dichlorobenzoyl)oxy)methyl ketone 9. The active site residues involved in the interaction are shown and the hydrogens are omitted for clarity.*

Ser339-NH...O=C- and -oxygen of Ser339 to back bone -NH of aspartate (1.97 Å) and is comparable with crystal structure, the distance is 2.30 Å. This type of hydrogen bonding was not present in hemiacetals. Two strong charge-charge type of hydrogen bonds are formed between Arg179-N and hydroxyl and -O- atoms of aspartyl carboxylate group. The dipeptide and tripeptide analogues (**10**, **11** and **12**) exhibit similar orientation with that of **9**, but the shift in 2,6-dichlorobenzoyloxy group positioned away from the active site by about 6 Å with Cys285, Val338, and Ser339 residues and show no hydrogen bond formation with the enzyme. The conformations differ largely at the **P1** site from that of ligand **9** which is nearly identical to that of crystal structure. The compound **9** has strong binding affinity -101.1 kcal/mol (Table 4) with the active site residues.

Regarding acetyl-Tyr-Val-Ala-Asp-[(2,6-[(bistrifluoromethyl)benzoyl]oxy]methyl ketone **13** built by taking ligand **5** as reference frame, the substitution of 2,6-(bistrifluoromethyl) benzoyloxy methyl fragment at **P1** site was positioned deep in the "oxyanion hole" consisting of Cys285 and Gly238 and formed two hydrogen bonds with Cys285. In one case aspartyl -NH formed hydrogen bond with SG atom of Cys285 (-NH-SG distance = 2.36 Å) and in the other a hydrogen bond between benzoyloxycarbonyl -C=O...HN of Cys285 was formed. The Gly238-NH...O=C- type of H-bonding was seen with **P1** aspartic acid. The 2,6-dimethyl substi-

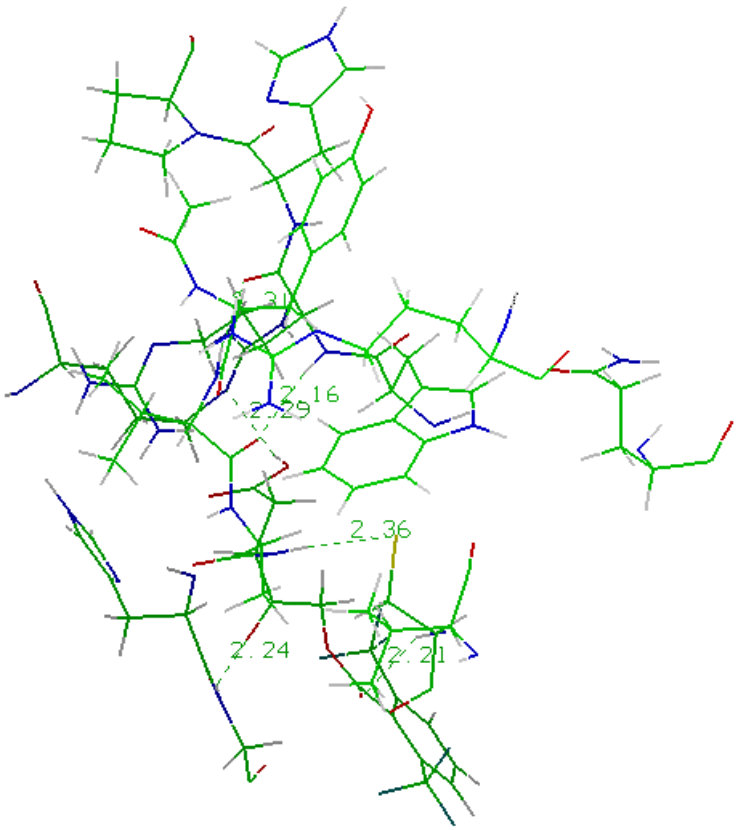

Figure 4. *The minimized energy structure of ICE/**13** complex in the final docking model. The dotted lines show potential hydrogen bonding interactions and numbers on the lines present distances (Å).*

tuted ligand **14** is unfavorable for interaction with oxyanion hole and is less active. This may be due to presence of high electron-withdrawing substituent (trifluoromethyl) in **13** made way for leaving group with the active site Cys285. The oxyanion of this inhibitor is stabilized by active site His237 which is located within the hydrogen bonding distance of 3.74 Å (Table 4) with the enzyme. It is assumed to be the stable conformation close to the crystal structure in which the aspartic acid OH group shifted to Arg179 and showed a strong hydrogen bonding interaction (OH...N-Arg179 distance = 2.29 Å) (Figure 4). The torsion angle 3 of O-C4-C5-CB varied about 27.5^0 due to the different substituent at **P1**. Compounds, phenylpropionyl peptidyl (acyloxy) methyl **15a** and **19a** (Table 3) showed higher binding energy than the (allyloxy)carbonyl (acyloxy)methyl ketones (**15b**, **20b**). These ligands were built from the complexed structure of **13** with the enzyme. The 2,6-bis (trifluoromethyl)benzoate leaving group did not involve in hydrogen bonding interaction with Cys285. The carbonyl leaving group positioned itself within the hydrogen bonding distance with Cys285 (2.70 Å). The ligand having the highest activity in (allyloxy)carbonyl (acyloxy)methyl ketone series **15b** built from **13** exhibited similar conformational orientation in the "oxyanion hole" to that of **13** and large change in the aspartic acid position was observed. The carboxylic acid group of aspartic acid oriented to **P1** site and participated in hydrogen bonding interaction with Cys285. The conformational flexibility in absence of **P4** Tyr moiety caused this type of interaction and has less binding energy. The structure of ICE reveals that Arg341, Arg179 and Gln383 form hydrogen bonds with O atom of alanine, carbonyl oxygen of leaving group and aspartic acid. These results suggest that **P4** Tyr is essential, while electron-withdrawing groups at 2,6 positions of leaving group are favorable for ICE inactivation but not the substituents of higher pKa values.

The RMS deviation was measured between the non-hydrogen atoms of the ICE/ligand in the docking model after energy-minimization and in the crystal structure of ICE (Table 4) to study the structural effects of ligand binding. The patterns of RMS difference produced by the ligand binding in the complex is similar for all three series and are in the range of 2.9-3.0 Å. The changes in binding energy is related to conformational rearrangements in the active site pocket of ICE induced by ligand with efficacies suggesting a correlation between the structural changes and activity variation.

Conclusions

By the use of a docking approach we have studied the binding mode of a series of aspartyl hemiacetals, α-((2,6-dichlorobenzoyl)oxy)methyl and (acyloxy)methyl ketones. In our model, O-benzylacyl of aspartyl hemiacetals is found to interact with Cys285 while semicarbazone and α-((2,6-dichlorobenzoyl) oxy)methyl groups of **P1** site protrude from the surface of Cys285 and interact with Val338, which is lo-

cated near the bottom of binding pocket. The intermolecular interaction energy results reveal the importance of **P1** site leaving groups for substrate specificity. The hydrogen bonding interactions with Cys285, Gly238 and His237 seem to play a crucial role for tight binding. In addition, the calculated RMS deviation pattern was similar in all ICE/ligand and suggest that the changes in binding energy is due to the ligand induced conformation within the active site. We suggest from these studies that the electron-withdrawing groups are desired for interaction with oxyanion hole but not the higher pKa values. Finally, the interaction energies of enzyme-inhibitor complexes calculated through docking and molecular dynamics simulations are in agreement with the reported experimental data, thus may be used for the rational design of more potent inhibitors of ICE.

Acknowledgement. Authors thank University Grants Commission (UGC) and All India Council for Technical Education (AICTE) for research grant.

Supplementary Material Available. Intermolecular hydrogen bond distances, conformational data analysis for compounds **5**, **7**, **9**, **13** and results of the binding mode of compound **7**, **15a** and **19a**.

References

1. Black, R. A.; Shirley, R.; Kronheim, R.; Sleath, P. R. *FEBS Lett*. **1989**, *247*, 386-390.
2. Kostura, M. J.; Tocci, M. J.; Limjuco, G.; Chin, J.; Cameron, P.; Hillman, A. G.; Chartrain, N. A.; Schmidt, J. A. *Proc. Natl. Acad. Sci*. **1989**, *86*, 5227-5231.
3. Thornberry, N. A.; Bull, H. G.; Calaycay, J. R.; Chapman K. T.; Howard, A. D.; Kostura, M. J.; Miller, D. K.; Molineaux, S. M.; Weidner, J. R.; Aunins, J.; Elliston, K. O.; Ayala, J. M.; Casano, F. J.; Chin, J.; Ding, G. J.-F.; Egger, L. A.; Gaffney, E. P.; Limjuco, G.; Palyha, O. C.; Raju, S. M.; Rolando, A. M.; Salley, J. P.; Yamin, T. T.; Lee, T. D.; Shively, J. E.; MacCross, M.; Mumford, R. A.; Schmidt, J. A.; Tocci, M. J. *Nature*. **1992**, *356*, 768-774.
4. Sleath, P. R.; Hendrickson, R. C.; Kronheim, S. R.; March, C. J.; Black, R. A. *J. Biol. Chem*. **1990**, *265*, 14526-14528.
5. Cerretti, D. P.; Kozlosky, C. J.; Mosley, B.; Nelson, N.; Ness, K. V.; Greenstreet, T. A.; March, C. J.; Kronheim, S. R.; Druck. T.; Cannizzaro, L. A.; Huebner, K.; Black, R. A. *Science*. **1992**, *256*, 97-100.
6. Howard, A. D.; Kostura, M. J.; Thornberry, N.; Ding, G. J.-F.; Limjuco, G.; Weidner, J.; Salley, J. P.; Hogquist, K. A.; Chaplin, D. D.; Mumford, R. A.; Schmidt, J. A.; Tocci, M. J. *J. Immunol*. **1991**, *147*, 29642969.
7. Molineaux, S. M.; Casano, F. J.; Rolando, A. M.; Peterson, E. P.; Limjuco, G.; Chin, J.; Griffin, P. R.; Calaycay J. R.; Ding, G. J.-F.; Yamin, T. T.; Palyha, O. C.; Luell, S.; Fletcher, D.; Miller, D. K.; Howard, A. D.; Thornberry, N, A.; Kostura, M. J. *Proc. Natl. Acad. Sci.* **1993**, *90*, 1809-1813.
8. Dinarello, C. A.; Wolff, S. M. *N. Eng. J. Med*. **1993**, *328*, 106.
9. Hannum, C. H.; Wilcox, C. J.; Arend, W. P.; Joslin, F. G.; Dripps, D. J.; Heimdal, P. L.; Armes, L. G.; Sommer, A.; Eisenberg, S. P.; Thompson, R. C. *Nature*. **1990**, *343*, 341-346.
10. Ohlsson, K.; Bjork, P.; Bergenfeldt, M.; Hageman, R.; Thompson, R. C. *Nature*. **1990**, *348*, 550-552.
11. Dinarello, C. A. *Blood*. **1991**, *77*, 1627.
12. Nicholson, D. W. *Nature Biotechnology*. **1996**, *14*, 297-301.
13. Smith, R. A.; Copp, L. J.; Donnelly, S. L.; Spencer, R. W.; Krantz, A. *Biochemistry*. **1988**, *27*, 6568-6573.
14. Krantz, A.; Copp, L. J.; Coles, P. J.; Smith, R. A.; Heard, S. B. *Biochemistry*. **1991**, *30*, 4678-4687.
15. Dolle, R. E.; Singh, J.; Rinker, J.; Hoyer, D.; Prasad, C. V. C.; Graybill, T. L.; Salviono, J. M.; Helaszek, C. T.; Miller, R.; Ator, M. A. *J. Med. Chem*. **1994**, *37*, 3863-3866.
16. Powers, J. C. In T*ransition-State and Mechanism-Based Inhibitors for Cysteine Protease*, 209th ACS National Meeting on Medicinal Chemistry, April 2-6, 1995, p 240.
17. Ator, M. A. In *Peptide and Nonpeptide Inhibitors of Interleukin-1 Beta Converting Enzyme*, 209th ACS National Meeting on Medicinal Chemistry, April 2-6, 1995, p 242.
18. Salvatore, M. J.; Hensens, O. D.; Zink, D. L.; Liesch, J.; Dufrense, C.; Ondeyka, J. G.; JÜrgens, T. M.; Borris, R. P.; Raghoobar, S.; McCauley, E.; Kong, L.; Gartner, S. E.; Koch, G. E.; Pelaéz, F.; Diez, M. T.; Cascales, C.; Martin, I.; Polishook, J. D.; Balick, M. J.; Beck, H. T.; King, S. R.; Hsu, A.; Lingham, R. B. *J. Nat. Products*. **1994**, *57*, 755-760.
19. Ray, C. A.; Black, R. A.; Kronheim, S. R.; Greenstreet, T. A.; Sleath, P. R.; Salvesen, G. S.; Pickup, D. J. *Cell*. **1992**, *69*, 597-604.
20. Wilson, K. P.; Black, Jo-Anne, F.; Thomson, J. A.; Kim, E. E.; Griffith, J. P.; Navia, M. A.; Murcko, M. A.; Chambers, S. P.; Aldape, R. A.; Raybuck, S. A.; Livingston D. J. *Nature*. **1994**, *370*, 270-275.
21. Walker, N. P. C.; Talanian, R. V.; Brady, K. D.; Dang, L. C.; Bump, N. J.; Ferenz, C. R.; Franklin, S.; Ghayur, T.; Hackett, M. C.; Hammill, L. D.; Herzog, L.; Hugunin, M.; Houy, W.; Mankovich, J. A.; McGuiness, L.; Oriewicz, E.; Paskind, M.; Pratt, C. A.; Reis, P.; Summani, A.; Terranova, M.; Welch, J. P.; Xiong, L.; Möller, A.; Tracey, D. E.; Kamen, R.; Wong, W. W. *Cell*. **1994**, *78*, 343-352.

22. Graybill, T. L.; Dolle, R. E.; Helaszek, C. T.; Miller, R. E.; Ator, M. A. *Int. J. Peptide Protein. Res*. **1994**, *1*, 1-10.
23. Thornberry, N. A.; Peterson, E. P.; Zhao, J. J.; Howard, A. D.; Griffin, P. R.; Chapman, K.T. *Biochemistry*. **1994**, *33*, 3934- 3940.
24. Dolle, R. E.; Hoyer, D.; Prasad, C. V. C.; Schmidt, J.; Helaszek, C.T.; Miller, R. E.; Ator, M. A. *J. Med. Chem*. **1994**, *37*, 563-564.
25. Chapman, K. T. *Biorg. Med. Chem*. **1992**, *2*, 613-618.
26. Hariprasad, V.; Kulkarni, V. M. J. Mol. Recogn. 1996, 9, 95-102.
27. Orozco, M.; Laughton, C. A.; Herzyk, P.; Neidle, S. *J. Biomol. Struct. Dyn*. **1990**, *8*, 359.
28. Hagler, A. T.; Lifson, S.; Dauber, P. *J. Am. Chem. Soc*. **1979a**, *101*, 5122-5130.
29. INSIGHT II ver. 2.3.5. Molecular Simulations Inc. 9685 Scranton Road, San Diego, 1994.

Table 1a. *hICE inhibitory activity of peptide aspartyl hemiacetals containing aspartyl aldehyde equivalents*

compound	structure	K_i(μM)
1	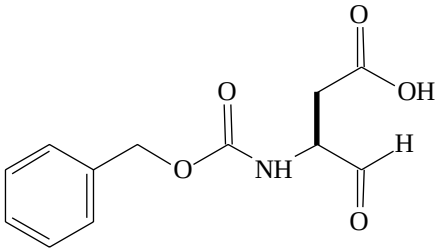	110
2	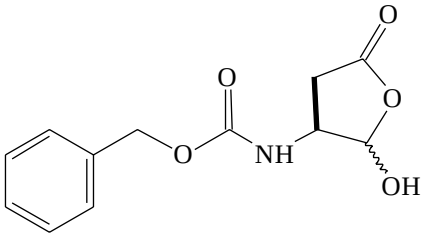	not available
3	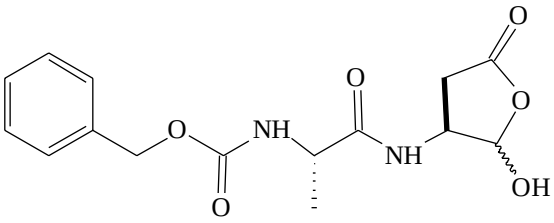	1.9
4	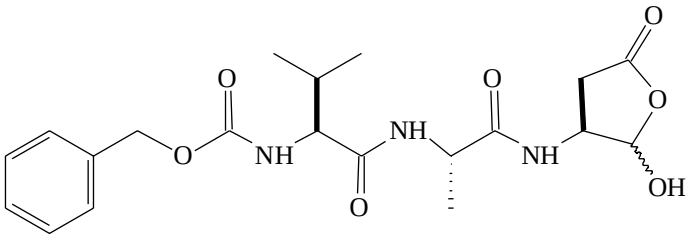	0.011
5	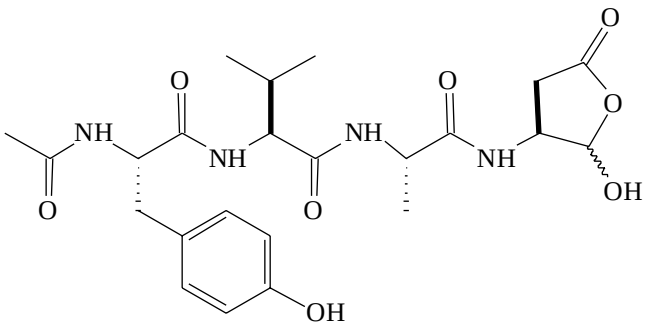	0.0072

Table 1b. *hICE inhibitory activity of peptide aspartyl hemiacetals containing aspartyl aldehyde equivalents*

compound	structure	K_i(μM)
6	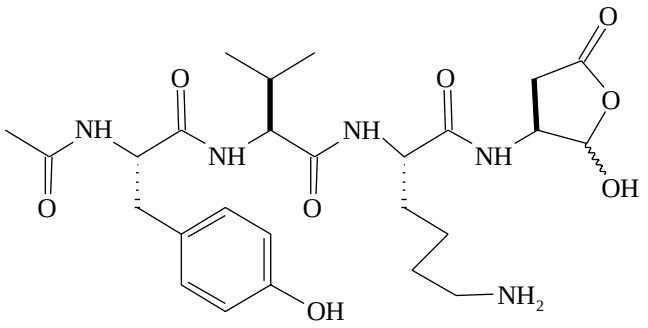	0.038
7	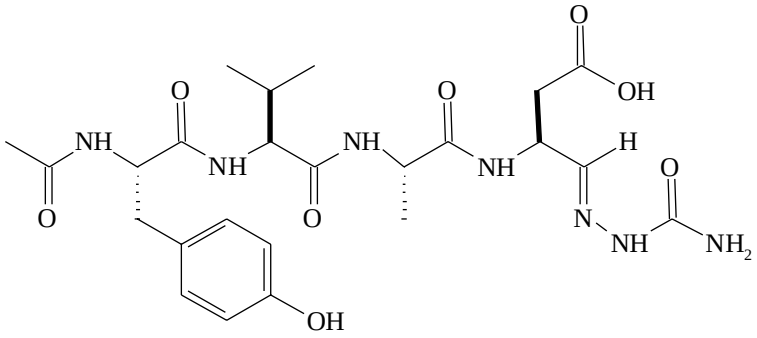	0.59
8	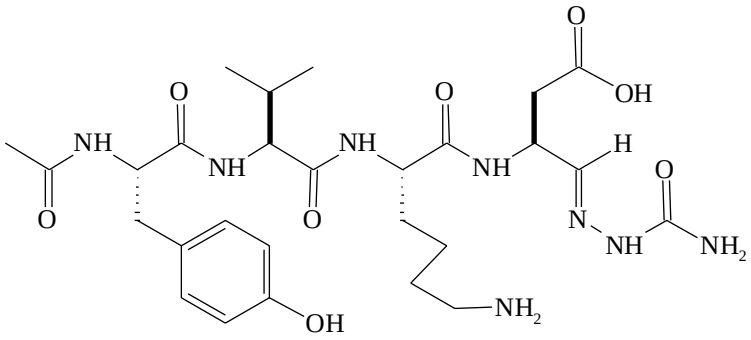	10

Table 2. *hICE inhibitory activity of α-(2,6-Dichlorobenzoyl)oxymethyl and (Acyloxy)methyl ketones*

compound	structure	($M^{-1}s^{-1}$)
9	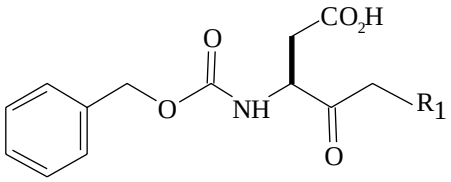	7.100 ± 200
10	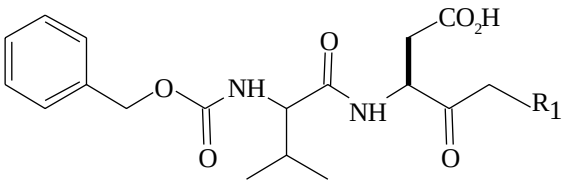	41.000 ± 700
11	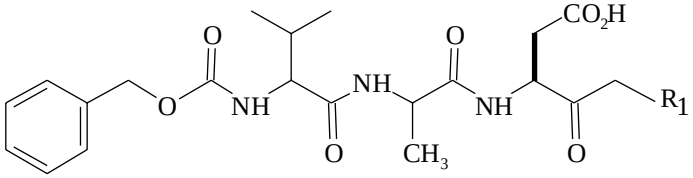	406.700 ± 38.400
12	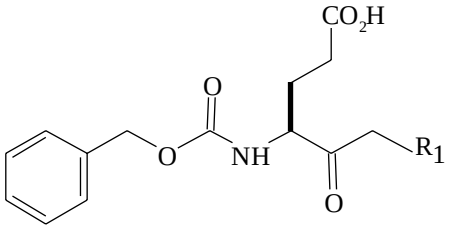	no inhibition at 20 mM
13	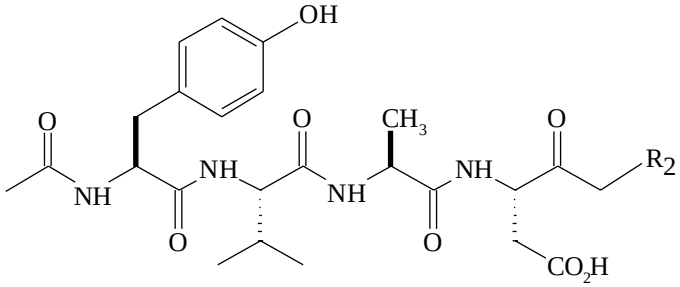	9.6×10^6
14	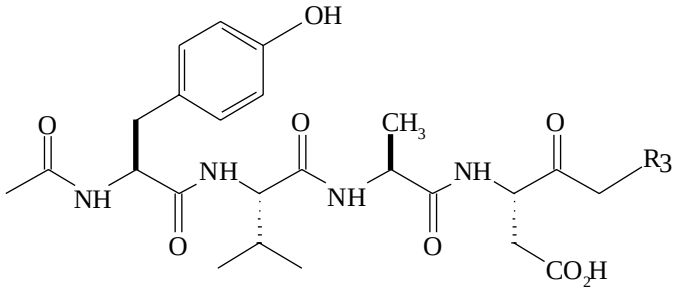	1×10^6

R_1= –O(C=O)-2,6-Cl_2Ph; R_2= –O(C=O)-2,6-$(CF_3)_2$Ph; R_3= –O(C=O)-2,6-$(CH_3)_2$Ph

Table 3. *hICE inactivation rate of peptide (Acyoxy)methyl ketone containing moieties*

		k ($M^{-1}s^{-1}$)	
	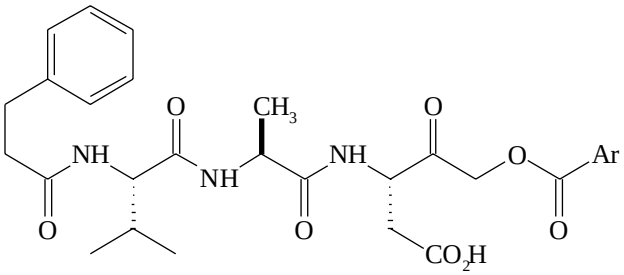 **a**	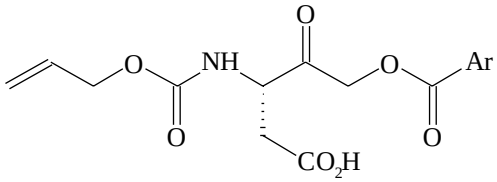 **b**	
compound	**Ar**		
15	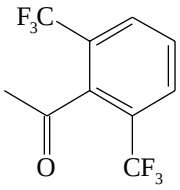	900,00	5,300
16	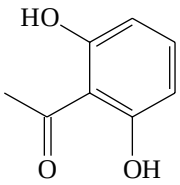	710,000	2,700
17	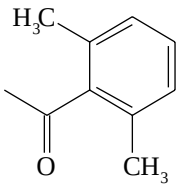	1,200,000	812
18	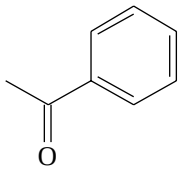	280,000	100
19	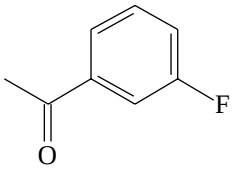	1,100,000	978
20	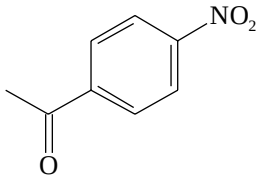	1,300,000	61

Table 4. *Energies of binding modes of ICE ligands (in kcal/mol) in the complex and stable docking states.*

ligand	total energy[a] (kcal/mol)	interaction[b] energy (kcal/mol)	K_i (μM)	k ($M^{-1}s^{-1}$)[c]	no. of H-bonds	rms [d]
4	192.5	-63.7	0.011	–	3	2.97
5	198.5	-66.5	0.0072	–	5	2.94
7	139.9	-73.6	0.59	–	11	3.02
9	208.5	-101.1	–	7,100 ± 200 4	3.09	
13	248.1	-118.1	–	9.6×10^6	6	3.00
15	302.3	-82.5	–	900 000	3	3.04
19	244.2	-91.1	–	1100 000	2	3.11
21	225.7	-64.2	–	5300	5	3.04

[a] The total energy includes the intermolecular energy (van der Waals and Coulomb energy) between hICE and the ligand.
[b] Intermolecular interaction energy between the hICE and ligand after minimization (kcal/mol).
[c] Second order rate constant for inactivation of ICE.
[d] rms deviation was measured between the non-hydrogen atoms of the ligand in the docking model after energy-minimization and in the crystal structure (2.82 Å).